

# Resistance of MMTV-NeuT/ATTAC mice to anti-PD-1 immune checkpoint therapy is associated with macrophage infiltration and Wnt pathway expression

Hongyan Yuan<sup>1</sup>, Lu Jin<sup>1</sup>, Handan Xiang<sup>2</sup>, Anannya Bhattacharya<sup>3</sup>, Philip E. Brandish<sup>3,4</sup>, Gretchen Baltus<sup>2</sup>, Alexander Tong<sup>1</sup>, Changyan Zhou<sup>1</sup> and Robert I. Glazer<sup>1</sup>

<sup>1</sup>Department of Oncology and Lombardi Comprehensive Cancer Center, Georgetown University Medical Center, Washington, DC 20007, USA

<sup>2</sup>Discovery Immunology, Merck Research Institute, Boston, MA 02115, USA

<sup>3</sup>Discovery Oncology, Merck Research Institute, Boston, MA 02115, USA

<sup>4</sup>Bicycle Therapeutics, Lexington, MA 02421, USA

**Correspondence to:** Robert I. Glazer, **email:** glazerr@georgetown.edu

**Keywords:** PD-1; NeuT; Wnt; macrophages; mammary tumorigenesis

**Received:** November 02, 2022

**Accepted:** December 07, 2022

**Published:** December 20, 2022

**Copyright:** © 2022 Yuan et al. This is an open access article distributed under the terms of the [Creative Commons Attribution License](https://creativecommons.org/licenses/by/3.0/) (CC BY 3.0), which permits unrestricted use, distribution, and reproduction in any medium, provided the original author and source are credited.

## ABSTRACT

**One of the central challenges for cancer therapy is the identification of factors in the tumor microenvironment that increase tumor progression and immune tolerance. In breast cancer, fibrosis is a histopathologic criterion for invasive cancer and poor survival that results from inflammatory factors and remodeling of the extracellular matrix to produce an immune tolerant microenvironment. To determine whether tolerance is associated with the immune checkpoint, Programmed Cell Death 1 (PD-1), NeuT/ATTAC mice, a conditional model of mammary fibrosis that we recently developed, were administered a murine-specific anti-PD-1 mAb related to pembrolizumab, and drug response was monitored by tumor development, imaging mass cytometry, immunohistochemistry and tumor gene expression by RNAseq. Tumor progression in NeuT/ATTAC mice was unaffected by weekly injection of anti-PD-1 over four months. Insensitivity to anti-PD-1 was associated with several processes, including increased tumor-associated macrophages (TAM), epithelial to mesenchymal transition (EMT), fibroblast proliferation, an enhanced extracellular matrix and the Wnt signaling pathway, including increased expression of Fzd5, Wnt5a, Vimentin, Mmp3, Col2a1 and Tgfβ1. These results suggest potential therapeutic avenues that may enhance PD-1 immune checkpoint sensitivity, including the use of tumor microenvironment targeted agents and Wnt pathway inhibitors.**

## INTRODUCTION

It has become increasingly apparent that the cell-centric hallmarks of cancer originally proposed [1] are exceedingly more complex, and must now take into account the multi-faceted role of multiple cell types in the tumor microenvironment (TME) [2–5]. Although the TME has emerged as an important determinant of tumorigenesis as well as a plausible therapeutic target [6], understanding the specific cellular and molecular changes in the TME

associated with breast cancer risk remains one of the overarching challenges for the prevention and treatment of this disease. Among the many stromal elements in the breast, adipose and fibrotic tissue comprise the largest components. Since stromal fibrosis is a histopathologic criterion of invasive breast cancer [7, 8], metastasis [9] and the development of precancerous lesions [10], identification of the signaling processes between tumor and stromal cells would greatly enhance our understanding of their roles in tumor progression. The TME undergoes

extensive changes during the transition from pre-invasive to invasive ductal breast carcinoma as a result of the paracrine effects of inflammatory factors elicited by tumor cells and cancer-associated fibroblasts and macrophages [11, 12]. Stromal fibroblasts secrete chemokines such as Cxcl1 which enhances tumor progression [13–15] by inhibiting the adaptive immune response through recruitment and activation of regulatory T cells (Treg) and myeloid-derived suppressor cells (MDSC) [16–20].

There have been relatively few animal models to study the relationship between mammary fibrosis and tumorigenesis. To address this objective, we utilized the ErbB2 transgenic model, MMTV-NeuT/ATTAC, where stromal fibrosis can be induced conditionally by the targeted ablation of mammary adipose tissue [21].

Utilizing this more stringent tumor model to test its susceptibility to anti-PD-1 immunotherapy, we report the signaling processes associated with its lack of responsiveness.

## RESULTS

### Fibrosis and tumor development

NeuT/ATTAC mice were used as a rigorous tumor model to test the efficacy of a murine-specific anti-PD-1 monoclonal antibody (mAb). Mice were treated with 100  $\mu$ g of the mAb or isotype-specific IgG twice weekly for four months and tumor development, tumor multiplicity and survival determined (Figure 1). Anti-PD-1

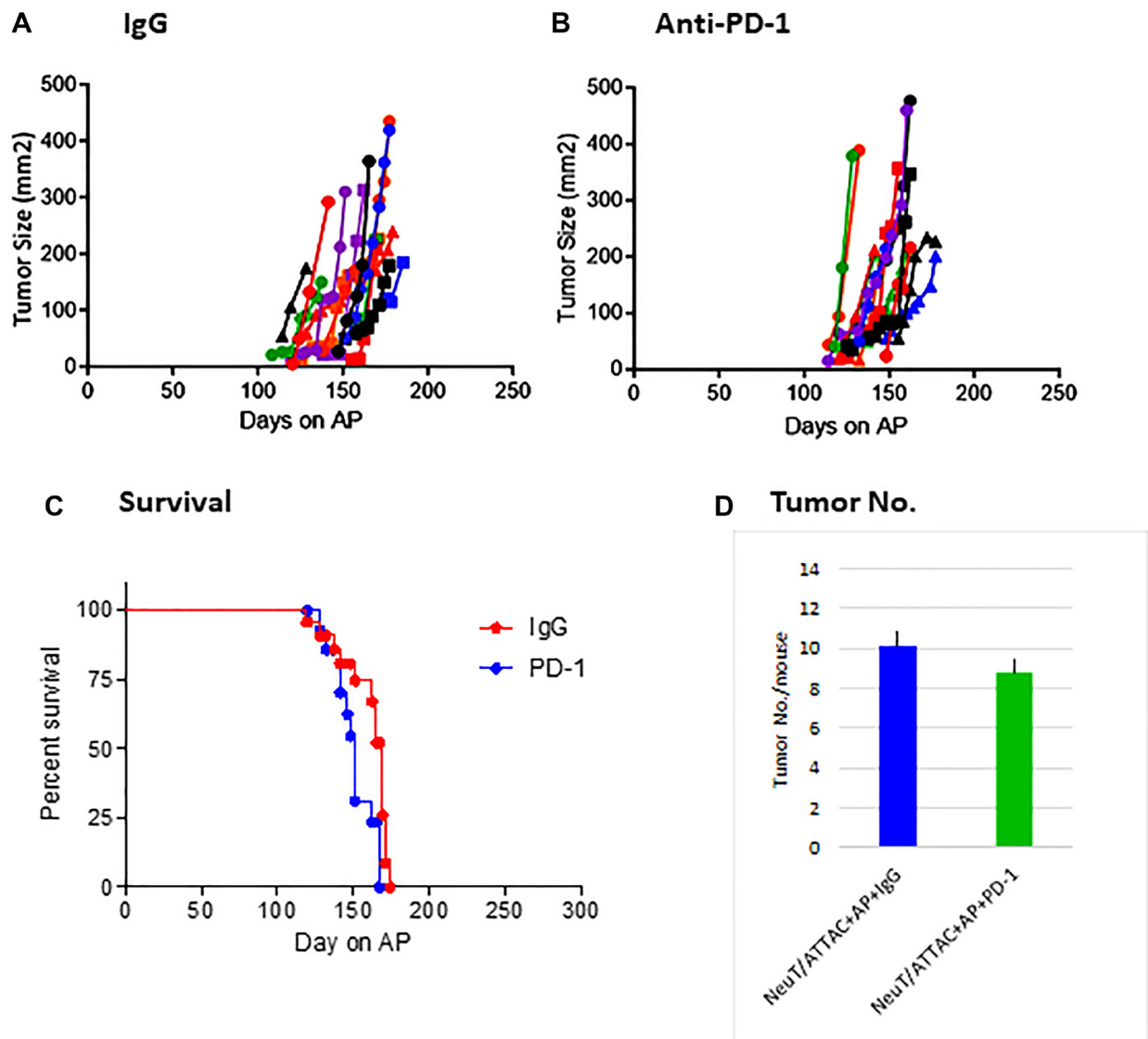


**Figure 1: Effect of anti-PD-1 mAb treatment on tumorigenesis in NeuT/ATTAC mice.** Tumor development in IgG-treated (A) and anti-PD-1-treated (B) mice over four months. Mice were treated triweekly by i.p. injection of 0.4 mg/kg AP21087 to induced fibrosis [21]. (C) Survival in NeuT/ATTAC mice. There was no significant difference between the IgG- and anti-PD-1-treated groups by the Mantel-Cox log-rank test. (D) Tumor multiplicity in NeuT/ATTAC mice after treatment with IgG or anti-PD-1. There was no significant difference ( $P > 0.05$ ) between the IgG- and anti-PD-1-treated groups by the two-sided Student's *t* test.

treatment did not affect these parameters, and therefore a detailed analysis of changes in the tumors and the immune environment were assessed to determine possible mechanisms for this lack of responsiveness.

IMC of tumors was used to evaluate changes in the TME (Figure 2). Similar cell types from IgG- and anti-PD-1-treated animals were grouped together (Figure 2A–2D). Ki67<sup>+</sup> proliferating cells were visualized predominantly

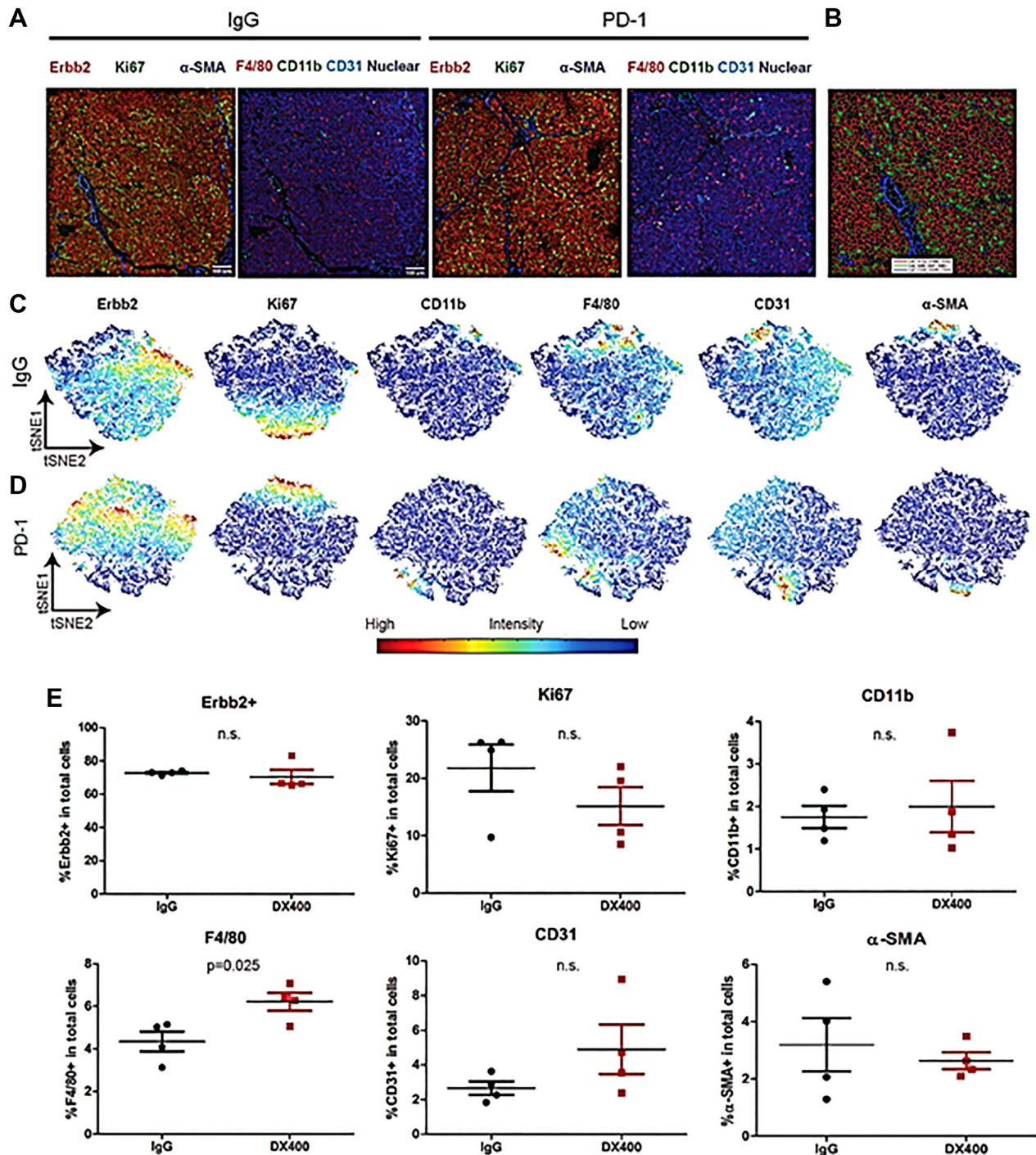


**Figure 2: Imaging mass cytometry of tumors from NeuT/ATTAC mice after treatment with anti-PD-1 or IgG.** Multiplex IHC and IMC was used to assess the effect of anti-PD-1 mAb treatment on the cellular composition of tumors from NeuT/ATTAC mice in which fibrosis was induced by AP21087 [21]. (A) Images of IgG and anti-PD-1-treated groups were obtained by staining with anti-ErbB2, -Ki67, -αSMA, -F4/80, -CD11b, and -CD31 antibodies. (B) Segmentation masks were generated for each image to visualize and quantify the cell types of interest into two dimensions [43]. (C, D) ErbB2<sup>+</sup>, Ki67<sup>+</sup>, CD11b<sup>+</sup>, F4/80<sup>+</sup>, CD31<sup>+</sup> and αSMA<sup>+</sup> cells were visualized in the IgG group and anti-PD-1 groups (*N* = 4 per group). (E) Quantification of the percentage of ErbB2<sup>+</sup>, Ki67<sup>+</sup>, CD11b<sup>+</sup>, F4/80<sup>+</sup>, CD31<sup>+</sup> and αSMA<sup>+</sup> cells from the IgG and anti-PD-1 groups. There was a significant increase in tumor-associated F4/80<sup>+</sup> macrophages (*p* < 0.025).

in  $ErbB2^+$  tumors, and anti-PD-1 mAb treatment did not alter the percentages of  $ErbB2^+$ ,  $Ki67^+$ ,  $CD11b^+$  monocytic myeloid cells,  $CD31^+$  endothelial cells or  $\alpha SMA^+$  fibroblasts/pericytes; however, a significant increase in tumor-associated  $F4/80^+$  macrophages ( $p < 0.025$ ) was observed (Figure 2E).

Analysis of tumor infiltrating immune cells by FACS indicated a significant increase of  $Foxp3^+/PD-1^-$  Treg cells, but no changes in the other cell subsets (Figure 3). To gain greater clarity about the processes associated with the insensitivity to anti-PD-1 therapy, transcriptomic analysis of the tumors was performed by RNAseq (Supplementary Table 1). Several processes were significantly upregulated, including myofibroblast differentiation, epithelial-to-mesenchymal transition (EMT), endothelial cell proliferation, ECM assembly, tumor growth and the Wnt pathway (Table 1). The latter pathway included increased expression of  $Fzd5$ ,  $Lef1$ ,  $Tgfb1$ ,  $Bmp1$ ,  $Mmp3$ ,  $Col2a1$  and  $Vim$ , and reduced expression of the  $Fzd5$  inhibitor  $Dkk1$  (Figure 4A, 4B). Increased protein expression of  $Fzd5$  and  $Vim$  and reduced expression of  $Dkk1$  were confirmed by IHC (Figure 4C).

## DISCUSSION

One of the impediments to successful cancer therapy is the heterogeneity and cellular plasticity of the tumor and TME [22, 23]. Using the NeuT/ATTAC fibrotic breast cancer model, we show that its unresponsiveness to anti-PD-1 therapy is associated in part with a gene network connected to increased expression of components of the Wnt pathway (Figure 4). These results are consistent with a previous study implicating the Wnt pathway in the lack of T cell expansion and resistance to anti-PD-1 therapy [24]. Similarly, the Wnt pathway has been shown to drive  $Tgfb1$  and  $Bmp1$  signaling [25, 26] and the promotion of a collagen-rich fibrotic phenotype that excludes T cell infiltration of the tumor [27, 28]. Interestingly, although the insensitivity to anti-PD-1 treatment in NeuT/ATTAC mice was associated with an increase in TAM (Figure 2), tumors exhibited a reduction in  $Arg1$  expression (Supplementary Table 1), which usually defines tissue macrophages with M1 polarization and sensitivity to immune checkpoint inhibitor therapy [29–31]. However, this may not reflect  $Arg1$  expression

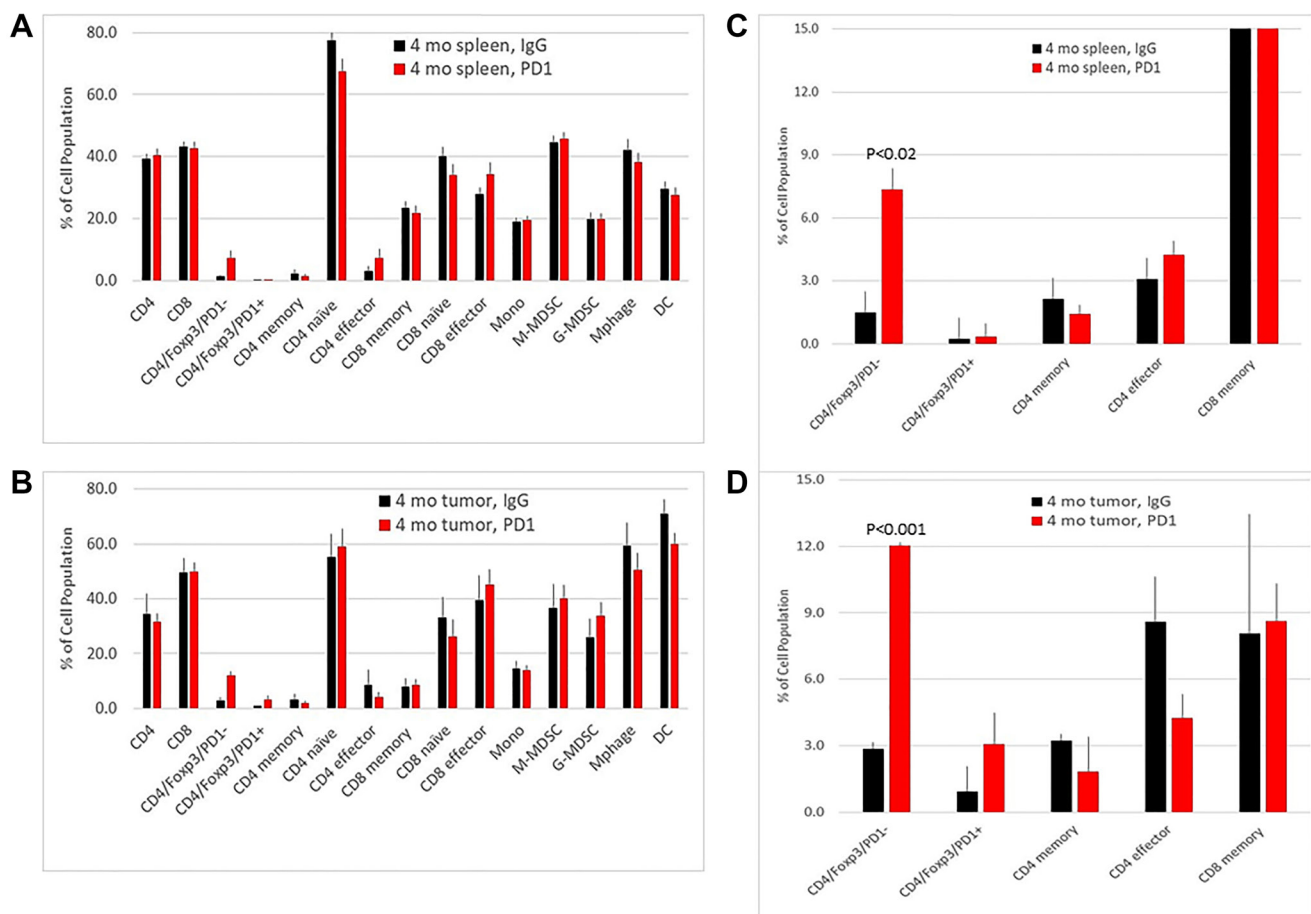


**Figure 3: Flow cytometry of immune cell subsets in spleen and tumors from NeuT/ATTAC mice after treatment with IgG or anti-PD-1.** FACS analysis of immune cells from spleen (A, B) and tumor infiltrates (C, D) after IgG and anti-PD-1 treatment. Panels B and D are presented on an expanded scale. There were significant increases in  $CD4^+/Foxp3^+/PD-1^-$  Treg cells in spleen ( $P < 0.02$ ) and tumors ( $P < 0.001$ ). Statistical significance was determined by the two-tailed Student's *t* test.



**Table 1: Transcriptomic analysis of the biological processes upregulated in tumors from NeuT/ATTAC+AP mice following anti-PD-1 treatment**

Gene set seed	Total # of Neighbors	Overlap	Overlapping entities	p-value
Myofibroblast differentiation	669	9	VCAN;CCN2;MMP3;BGN;PLAUR;VIM;TERT;WNT5A;TGFB1	5.00E-10
Mesenchymal stem cell differentiation	850	9	VCAN;CCN2;COL2A1;PLAUR;CCND1;LEF1;TERT;WNT5A;TGFB1	5.15E-09
Canonical Wnt signaling pathway	2592	13	CCN2;MMP3;PLAUR;VIM;CCND1;LEF1;TERT;WNT5A;VCAN;COL2A1;BGN;FZD5;TGFB1	7.06E-09
Fibroblast proliferation	1278	10	VCAN;CCN2;MMP3;BGN;PLAUR;VIM;CCND1;TERT;WNT5A;TGFB1	1.43E-08
Endothelial cell proliferation	1766	11	CCN2;MMP3;PLAUR;VIM;CCND1;TERT;WNT5A;VCAN;BGN;BMP1;TGFB1	2.59E-08
Smooth muscle cell migration	749	9	VCAN;CCN2;MMP3;BGN;PLAUR;VIM;CCND1;WNT5A;TGFB1	3.75E-08
Fibrogenesis	1091	9	VCAN;CCN2;MMP3;BGN;PLAUR;VIM;CCND1;WNT5A;TGFB1	5.70E-08
ECM assembly	881	8	VCAN;CCN2;COL2A1;BGN;VIM;WNT5A;BMP1;TGFB1	1.52E-07
Tumor cell growth	2081	11	CCN2;MMP3;PLAUR;VIM;CCND1;LEF1;TERT;WNT5A;VCAN;BGN;TGFB1	1.69E-07
Macrophage infiltration	1086	9	CCN2;COL2A1;MMP3;BGN;PLAUR;VIM;TERT;WNT5A;TGFB1	9.12E-07

Shown are processes based on a  $\geq 1.5\times$  increase in RNA expression with a  $p$ -value  $< 0.05$  (Supplementary Table 1) using Pathway Studio v. 9.

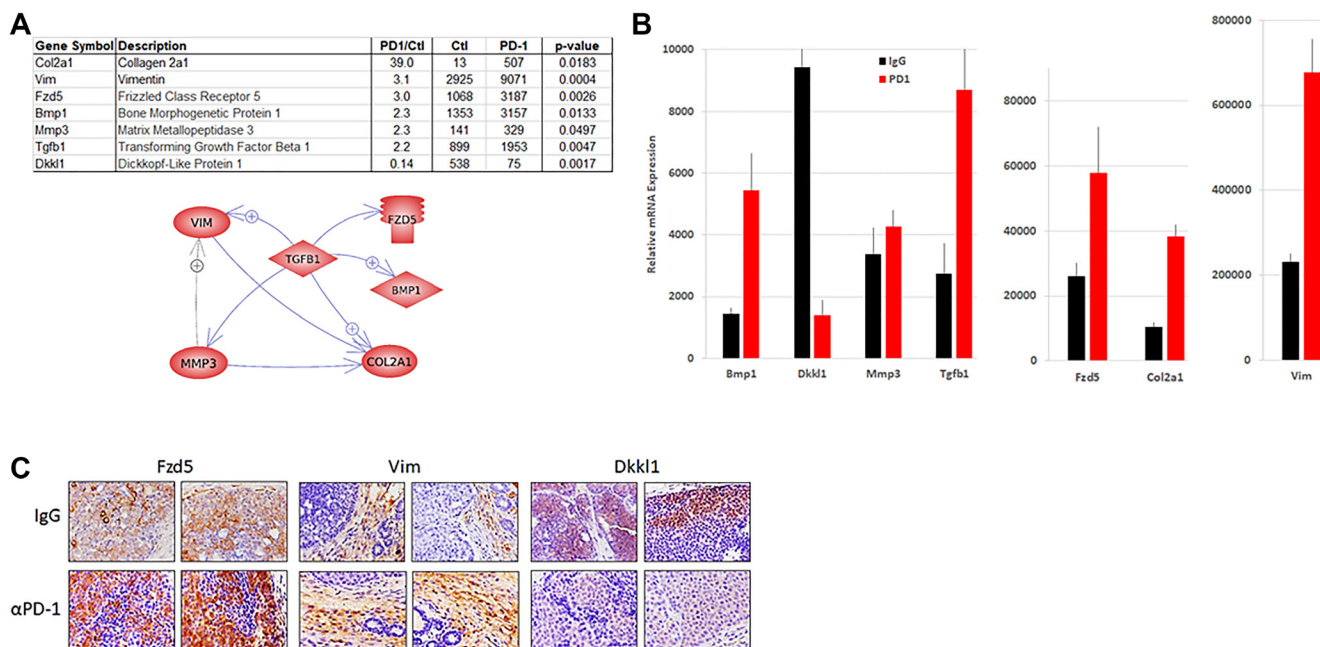


**Figure 4: Wnt pathway expression in tumors from NeuT/ATTAC mice.** RNA was prepared from mammary tumors from each group ( $N = 5$ ) and pooled for RNAseq. (A) Wnt pathway genes that were upregulated in anti-PD-1-treated mice. Gene interactions were determined with Pathway Studio version 9.1. (B) qRT-PCR analysis of the genes in (A). (C) IHC of Wnt pathway components in tumors of NeuT/ATTAC mice.

in TAM, which do not exhibit the distinct functionality of tissue macrophages [32].

Although the present study was conducted in AP-21087-treated NeuT/ATTAC FVB mice and not in untreated mice, previous studies have shown that MMTV-NeuT Balb/c mice were insensitive to anti-PD-1 treatment [33] and failed to generate a cytotoxic T cell response to anti-erbB2 therapy [34], suggesting that the NeuT genotype is immune suppressed.

Lastly, among all of the tumor-infiltrating immune cell subsets, only Foxp3<sup>+</sup>/PD-1<sup>-</sup> Treg cells were elevated (Figure 3), a subset known to be more immunosuppressive than Foxp3<sup>+</sup>/PD-1<sup>+</sup> Treg cells [35] and a phenotype expected to be intrinsically insensitive to anti-PD-1 mAb.

Overall, the immune tolerant TME in NeuT/ATTAC mice was associated with tumor-infiltrating macrophages, Foxp3<sup>+</sup>/PD-1<sup>-</sup> Treg cells as well as upregulation of the Wnt signaling pathway, which may provide further insights into the therapeutic options that may enhance immune checkpoint therapy.

## MATERIALS AND METHODS

### Animals

MMTV-NeuT mice [36] were obtained from Jackson Labs (FVB-Tg(MMTV-ErbB2)NK1Mul/J) [37] and FAT-ATTAC mice on a C57BL/6 background were kindly provided by Dr. Philipp Scherer, University of Texas Southwestern [38, 39]. FAT-ATTAC mice were crossed into the FVB strain and subsequently with MMTV-NeuT mice to produce NeuT/ATTAC mice as previously described [21]. In brief, NeuT/ATTAC mice at 6 weeks of age were injected i.p. triweekly with 0.4 mg/kg AP20187 throughout tumor development to induce fibrosis [21]. At 8 weeks of age, mice were injected i.p. twice weekly with 100 µg of the anti-PD-1 monoclonal antibody (mAb) or a matching isotype-specific IgG mAb for four months. This dose achieved a plasma level of 36 ± 3.6 µg/ml (mean ± S.E., *N* = 21), suggesting even distribution in total blood volume (unpublished results). All treatments and tumor measurements were carried out by Carlos Benitez and Maria Idalia Cruz under the auspices of the Animal Shared Resource.

### Fluorescence-activated cell sorting (FACS)

Tumor and spleen were removed and digested with collagenase D (Roche) and the cell suspension filtered, washed and erythrocytes lysed before analysis of 1 × 10<sup>6</sup> cells by FACS as previously described [15]. Viable cells were determined with the Live/Dead Fixable Dead Cell Stain Kit (Invitrogen) and excluded from analysis, and non-specific binding was blocked with Fc antibody CD16/32 (Biolegend). Cells were sorted for CD45<sup>+</sup> cells

and subsequently for macrophages (F4/80<sup>+</sup>/MHCII<sup>+</sup>), G-MDSC (CD11b<sup>+</sup>/Gr-1<sup>+</sup>), M-MDSC (CD11b<sup>+</sup>/Ly6C<sup>+</sup>), dendritic cells (CD11c<sup>+</sup>/MHCII<sup>+</sup>), T cells (CD4<sup>+</sup>/CD8<sup>+</sup>), NK cells (CD45<sup>+</sup>/NK1.1<sup>+</sup>) and Treg cells (Foxp3<sup>+</sup>/PD-1) as previously described [15, 21]. Analysis was conducted by the Flow Cytometry and Cell Sorting Shared Resource using a BD LSRFortessa analyzer (BD Biosciences) and FCS Express 4 software (De Novo Software). Antibodies and their dilutions are listed in Supplementary Table 2.

### Histopathology and immunohistochemistry

Mammary tissue was excised and FFPE sections were prepared for antigen retrieval as previously described [40, 41]. Biotin-conjugated secondary antibodies were diluted in TBS containing 0.1% Tween-20 and incubated for 30 min at room temperature using ABC Vectastain (Vector Laboratories) and diaminobenzidine (Pierce). Slides were counterstained with Harris-modified hematoxylin (Thermo-Fisher, Inc.), dehydrated and mounted in Permount (Thermo-Fisher, Inc.). Antibodies and their dilutions are listed in Supplementary Table 2.

### RNAseq analysis

RNA was extracted, its quality assessed and RNAseq performed by Novogene as previously described [21, 42]. Raw data quality was checked using FastQC (v0.11.9), and adapter trimming of raw data was performed using Cutadapt (v3.5). The reference genome was downloaded from Ensembl mm10 release 99, and the reference genome index was built using Bowtie2 (v2.4.1) software. Paired-end trimmed reads alignment and raw read count calculation were performed using RSEM software (v1.3.1). Statistical analysis was performed using the DESeq2 package (v1.36.0) in R (v4.1). Genes with *p*-value < 0.05 were considered as differentially expressed and used as input for Gene Set Enrichment Analysis (GSEA) (v4.2.3, Broad Institute). RNAseq data were deposited in the GEO database under accession no. GSE215964.

### Quantitative real-time polymerase chain reaction (qRT-PCR)

Total RNA (1 µg) from each of 3 samples per group was reverse transcribed using the Omniscript RT kit (Qiagen) as previously described [21, 41]. PCR was performed in triplicate using an ABI-Prism 7700 (Applied Biosystems) and SYBRGreen I detection (Qiagen) according to the manufacturer's protocol. Amplification using the appropriate primers was confirmed by ethidium bromide staining of the PCR products on an agarose gel. The expression of each target gene was normalized to

GAPDH and is presented as the ratio of the target gene to GAPDH expression calculated using the formula,  $2^{-\Delta Ct}$ , where  $\Delta Ct = Ct^{\text{Target}} - Ct^{18s}$  [41]. RT-PCR primers are listed in Supplementary Table 3.

### Imaging mass cytometry (IMC)

Multiplex IHC and IMC was used to assess the effect of anti-PD-1 mAb treatment on the cellular composition of tumors from NeuT/ATTAC mice ( $N = 4$  per group) after induction of fibrosis by AP21087 [21]. Twenty-four tumor, stromal and immune cell markers were tested, and six positive signals were obtained (Figure 2A). Segmentation masks were generated for each image to enable single cell data extraction with histoCAT software to visualize and quantify the cell types of interest [43]. T-SNE, a multidimensional reduction tool, was used to generate single cell data into two dimensions. A list of antibodies is provided in Supplementary Table 2.

### Statistical analysis

Statistical significance of means  $\pm$  S.E. were evaluated using the two-tailed Student's *t* test at a significance of  $P < 0.05$ . Survival data were analyzed using the Mantel-Cox log-rank test and tumor growth by the unpaired two-tailed Student's *t* test at a significance of  $P < 0.05$  using Prism GraphPad software.

### Author contributions

Conceptualization: Robert I. Glazer and Philip E. Brandish. Data curation and methodology: Hongyan Yuan, Lu Jin, Hondan Xiang, Anannya Bhattacharya, Alexander Tong. Writing original draft: Robert I. Glazer. Project administration: Robert I. Glazer and Philip E. Brandish. Funding acquisition: Robert I. Glazer, Gretchen Baltus and Philip E. Brandish.

### ACKNOWLEDGMENTS

This work was supported by a contract from the Research Institute of Merck and Co., Inc., Rahway, NJ, USA to R.I.G. and award 1P30 CA051008 from the National Cancer Institute, NIH, to the Lombardi Comprehensive Cancer Center. This investigation was conducted using the Animal Research, Genomics and Epigenomics, Histology and Tissue, Flow Cytometry and Microscopy and Imaging Shared Resources of Georgetown University, and by an animal facilities construction grant from the NIH.

### CONFLICTS OF INTEREST

Authors have no conflicts of interest to declare.

### Ethical statement

All animal studies were conducted under protocol 2016-1143 approved by the Georgetown University Animal Care and Use Committee in accordance with NIH guidelines for the ethical treatment of animals.

### REFERENCES

1. Hanahan D, Weinberg RA. The hallmarks of cancer. *Cell*. 2000; 100:57–70. [https://doi.org/10.1016/s0092-8674\(00\)81683-9](https://doi.org/10.1016/s0092-8674(00)81683-9). [PubMed]
2. Polyak K, Haviv I, Campbell IG. Co-evolution of tumor cells and their microenvironment. *Trends Genet*. 2009; 25:30–38. <https://doi.org/10.1016/j.tig.2008.10.012>. [PubMed]
3. Pietras K, Ostman A. Hallmarks of cancer: interactions with the tumor stroma. *Exp Cell Res*. 2010; 316:1324–31. <https://doi.org/10.1016/j.yexcr.2010.02.045>. [PubMed]
4. Hanahan D, Coussens LM. Accessories to the crime: functions of cells recruited to the tumor microenvironment. *Cancer Cell*. 2012; 21:309–22. <https://doi.org/10.1016/j.ccr.2012.02.022>. [PubMed]
5. Hanahan D, Weinberg RA. Hallmarks of cancer: the next generation. *Cell*. 2011; 144:646–74. <https://doi.org/10.1016/j.cell.2011.02.013>. [PubMed]
6. Tchou J, Conejo-Garcia J. Targeting the tumor stroma as a novel treatment strategy for breast cancer: shifting from the neoplastic cell-centric to a stroma-centric paradigm. *Adv Pharmacol*. 2012; 65:45–61. <https://doi.org/10.1016/B978-0-12-397927-8.00003-8>. [PubMed]
7. Van den Eynden GG, Colpaert CG, Couvelard A, Pezzella F, Dirix LY, Vermeulen PB, Van Marck EA, Hasebe T. A fibrotic focus is a prognostic factor and a surrogate marker for hypoxia and (lymph)angiogenesis in breast cancer: review of the literature and proposal on the criteria of evaluation. *Histopathology*. 2007; 51:440–51. <https://doi.org/10.1111/j.1365-2559.2007.02761.x>. [PubMed]
8. Gill JK, Maskarinec G, Pagano I, Kolonel LN. The association of mammographic density with ductal carcinoma in situ of the breast: the Multiethnic Cohort. *Breast Cancer Res*. 2006; 8:R30. <https://doi.org/10.1186/bcr1507>. [PubMed]
9. Hasebe T. Tumor-stromal interactions in breast tumor progression--significance of histological heterogeneity of tumor-stromal fibroblasts. *Expert Opin Ther Targets*. 2013; 17:449–60. <https://doi.org/10.1517/14728222.2013.757305>. [PubMed]
10. Boyd NF, Martin LJ, Bronskill M, Yaffe MJ, Duric N, Minkin S. Breast tissue composition and susceptibility to breast cancer. *J Natl Cancer Inst*. 2010; 102:1224–37. <https://doi.org/10.1093/jnci/djq239>. [PubMed]
11. Park J, Scherer PE. Leptin and cancer: from cancer stem cells to metastasis. *Endocr Relat Cancer*. 2011; 18:C25–29. <https://doi.org/10.1530/ERC-11-0163>. [PubMed]

12. Zheng Q, Dunlap SM, Zhu J, Downs-Kelly E, Rich J, Hursting SD, Berger NA, Reizes O. Leptin deficiency suppresses MMTV-Wnt-1 mammary tumor growth in obese mice and abrogates tumor initiating cell survival. *Endocr Relat Cancer*. 2011; 18:491–503. <https://doi.org/10.1530/ERC-11-0102>. [PubMed]
13. Orimo A, Gupta PB, Sgroi DC, Arenzana-Seisdedos F, Delaunay T, Naeem R, Carey VJ, Richardson AL, Weinberg RA. Stromal fibroblasts present in invasive human breast carcinomas promote tumor growth and angiogenesis through elevated SDF-1/CXCL12 secretion. *Cell*. 2005; 121:335–48. <https://doi.org/10.1016/j.cell.2005.02.034>. [PubMed]
14. Acharyya S, Oskarsson T, Vanharanta S, Malladi S, Kim J, Morris PG, Manova-Todorova K, Leversha M, Hogg N, Seshan VE, Norton L, Brogi E, Massagué J. A CXCL1 paracrine network links cancer chemoresistance and metastasis. *Cell*. 2012; 150:165–78. <https://doi.org/10.1016/j.cell.2012.04.042>. [PubMed]
15. Yuan H, Wang X, Shi C, Jin L, Hu J, Zhang A, Li J, Vijayendra N, Doodala V, Weiss S, Tang Y, Weiner LM, Glazer RI. Plac1 Is a Key Regulator of the Inflammatory Response and Immune Tolerance In Mammary Tumorigenesis. *Sci Rep*. 2018; 8:5717. <https://doi.org/10.1038/s41598-018-24022-w>. [PubMed]
16. Grivennikov SI, Greten FR, Karin M. Immunity, inflammation, and cancer. *Cell*. 2010; 140:883–99. <https://doi.org/10.1016/j.cell.2010.01.025>. [PubMed]
17. Mellman I, Coukos G, Dranoff G. Cancer immunotherapy comes of age. *Nature*. 2011; 480:480–89. <https://doi.org/10.1038/nature10673>. [PubMed]
18. Pardoll DM. The blockade of immune checkpoints in cancer immunotherapy. *Nat Rev Cancer*. 2012; 12:252–64. <https://doi.org/10.1038/nrc3239>. [PubMed]
19. Jamieson T, Clarke M, Steele CW, Samuel MS, Neumann J, Jung A, Huels D, Olson MF, Das S, Nibbs RJ, Sansom OJ. Inhibition of CXCR2 profoundly suppresses inflammation-driven and spontaneous tumorigenesis. *J Clin Invest*. 2012; 122:3127–44. <https://doi.org/10.1172/JCI61067>. [PubMed]
20. Highfill SL, Cui Y, Giles AJ, Smith JP, Zhang H, Morse E, Kaplan RN, Mackall CL. Disruption of CXCR2-mediated MDSC tumor trafficking enhances anti-PD1 efficacy. *Sci Transl Med*. 2014; 6:237ra67. <https://doi.org/10.1126/scitranslmed.3007974>. [PubMed]
21. Yuan H, Wang X, Lu J, Zhang Q, Brandina I, Alexandrov I, Glazer RI. MMTV-NeuT/ATTAC mice: a new model for studying the stromal tumor microenvironment. *Oncotarget*. 2018; 9:8042–53. <https://doi.org/10.18632/oncotarget.24233>. [PubMed]
22. Marusyk A, Janiszewska M, Polyak K. Intratumor Heterogeneity: The Rosetta Stone of Therapy Resistance. *Cancer Cell*. 2020; 37:471–84. <https://doi.org/10.1016/j.ccell.2020.03.007>. [PubMed]
23. Huo X, Li H, Li Z, Yan C, Agrawal I, Mathavan S, Liu J, Gong Z. Transcriptomic profiles of tumor-associated neutrophils reveal prominent roles in enhancing angiogenesis in liver tumorigenesis in zebrafish. *Sci Rep*. 2019; 9:1509. <https://doi.org/10.1038/s41598-018-36605-8>. [PubMed]
24. Bassez A, Vos H, Van Dyck L, Floris G, Arijs I, Desmedt C, Boeckx B, Vanden Bempt M, Nevelsteen I, Lambein K, Punie K, Neven P, Garg AD, et al. A single-cell map of intratumoral changes during anti-PD1 treatment of patients with breast cancer. *Nat Med*. 2021; 27:820–32. <https://doi.org/10.1038/s41591-021-01323-8>. [PubMed]
25. Cheng N, Bhowmick NA, Chytil A, Gorksa AE, Brown KA, Muraoka R, Arteaga CL, Neilson EG, Hayward SW, Moses HL. Loss of TGF-beta type II receptor in fibroblasts promotes mammary carcinoma growth and invasion through upregulation of TGF-alpha-, MSP- and HGF-mediated signaling networks. *Oncogene*. 2005; 24:5053–68. <https://doi.org/10.1038/sj.onc.1208685>. [PubMed]
26. Browning LM, Pietrzak M, Kuczma M, Simms CP, Kurczewska A, Refugia JM, Lowery DJ, Rempala G, Gutkin D, Ignatowicz L, Muranski P, Kraj P. TGF-β-mediated enhancement of T<sub>H</sub>17 cell generation is inhibited by bone morphogenetic protein receptor 1α signaling. *Sci Signal*. 2018; 11:eaar2125. <https://doi.org/10.1126/scisignal.aar2125>. [PubMed]
27. Román-Pérez E, Casbas-Hernández P, Pirone JR, Rein J, Carey LA, Lubet RA, Mani SA, Amos KD, Troester MA. Gene expression in extratumoral microenvironment predicts clinical outcome in breast cancer patients. *Breast Cancer Res*. 2012; 14:R51. <https://doi.org/10.1186/bcr3152>. [PubMed]
28. Mariathasan S, Turley SJ, Nickles D, Castiglioni A, Yuen K, Wang Y, Kadel EE III, Koepfen H, Astarita JL, Cubas R, Jhunjunwala S, Banchereau R, Yang Y, et al. TGFβ attenuates tumour response to PD-L1 blockade by contributing to exclusion of T cells. *Nature*. 2018; 554:544–48. <https://doi.org/10.1038/nature25501>. [PubMed]
29. Qian BZ, Pollard JW. Macrophage diversity enhances tumor progression and metastasis. *Cell*. 2010; 141:39–51. <https://doi.org/10.1016/j.cell.2010.03.014>. [PubMed]
30. Wang N, Liang H, Zen K. Molecular mechanisms that influence the macrophage m1-m2 polarization balance. *Front Immunol*. 2014; 5:614. <https://doi.org/10.3389/fimmu.2014.00614>. [PubMed]
31. Arlauckas SP, Garren SB, Garris CS, Kohler RH, Oh J, Pittet MJ, Weissleder R. Arg1 expression defines immunosuppressive subsets of tumor-associated macrophages. *Theranostics*. 2018; 8:5842–54. <https://doi.org/10.7150/thno.26888>. [PubMed]
32. Franklin RA, Liao W, Sarkar A, Kim MV, Bivona MR, Liu K, Pamer EG, Li MO. The cellular and molecular origin of tumor-associated macrophages. *Science*. 2014; 344:921–25. <https://doi.org/10.1126/science.1252510>. [PubMed]
33. Workenhe ST, Nguyen A, Bakhshinyan D, Wei J, Hare DN, MacNeill KL, Wan Y, Oberst A, Bramson JL, Nasir JA, Vito A, El-Sayes N, Singh SK, et al. De novo necroptosis



- creates an inflammatory environment mediating tumor susceptibility to immune checkpoint inhibitors. *Commun Biol.* 2020; 3:645. <https://doi.org/10.1038/s42003-020-01362-w>. [PubMed]
34. Melani C, Chiodoni C, Forni G, Colombo MP. Myeloid cell expansion elicited by the progression of spontaneous mammary carcinomas in c-erbB-2 transgenic BALB/c mice suppresses immune reactivity. *Blood.* 2003; 102:2138–45. <https://doi.org/10.1182/blood-2003-01-0190>. [PubMed]
35. Tan CL, Kuchroo JR, Sage PT, Liang D, Francisco LM, Buck J, Thaker YR, Zhang Q, McArdel SL, Juneja VR, Lee SJ, Lovitch SB, Lian C, et al. PD-1 restraint of regulatory T cell suppressive activity is critical for immune tolerance. *J Exp Med.* 2021; 218:e20182232. <https://doi.org/10.1084/jem.20182232>. [PubMed]
36. Muller WJ, Sinn E, Pattengale PK, Wallace R, Leder P. Single-step induction of mammary adenocarcinoma in transgenic mice bearing the activated c-neu oncogene. *Cell.* 1988; 54:105–15. [https://doi.org/10.1016/0092-8674\(88\)90184-5](https://doi.org/10.1016/0092-8674(88)90184-5). [PubMed]
37. Guy CT, Cardiff RD, Muller WJ. Induction of mammary tumors by expression of polyomavirus middle T oncogene: a transgenic mouse model for metastatic disease. *Mol Cell Biol.* 1992; 12:954–61. <https://doi.org/10.1128/mcb.12.3.954-961.1992>. [PubMed]
38. Landskroner-Eiger S, Park J, Israel D, Pollard JW, Scherer PE. Morphogenesis of the developing mammary gland: stage-dependent impact of adipocytes. *Dev Biol.* 2010; 344:968–78. <https://doi.org/10.1016/j.ydbio.2010.06.019>. [PubMed]
39. Pajvani UB, Trujillo ME, Combs TP, Iyengar P, Jelicks L, Roth KA, Kitsis RN, Scherer PE. Fat apoptosis through targeted activation of caspase 8: a new mouse model of inducible and reversible lipodystrophy. *Nat Med.* 2005; 11:797–803. <https://doi.org/10.1038/nm1262>. [PubMed]
40. Yuan H, Lu J, Xiao J, Upadhyay G, Umans R, Kallakury B, Yin Y, Fant ME, Kopelovich L, Glazer RI. PPAR $\delta$  induces estrogen receptor-positive mammary neoplasia through an inflammatory and metabolic phenotype linked to mTOR activation. *Cancer Res.* 2013; 73:4349–61. <https://doi.org/10.1158/0008-5472.CAN-13-0322>. [PubMed]
41. Upadhyay G, Yin Y, Yuan H, Li X, Derynck R, Glazer RI. Stem cell antigen-1 enhances tumorigenicity by disruption of growth differentiation factor-10 (GDF10)-dependent TGF-beta signaling. *Proc Natl Acad Sci U S A.* 2011; 108:7820–25. <https://doi.org/10.1073/pnas.1103441108>. [PubMed]
42. Sheng G, Yuan H, Jin L, Ranjit S, Panov J, Lu X, Levi M, Glazer RI. Reduction of fibrosis and immune suppressive cells in ErbB2-dependent tumorigenesis by an LXR agonist. *PLoS One.* 2021; 16:e0248996. <https://doi.org/10.1371/journal.pone.0248996>. [PubMed]
43. Schapiro D, Jackson HW, Raghuraman S, Fischer JR, Zanolli VRT, Schulz D, Giesen C, Catena R, Varga Z, Bodenmiller B. histoCAT: analysis of cell phenotypes and interactions in multiplex image cytometry data. *Nat Methods.* 2017; 14:873–76. <https://doi.org/10.1038/nmeth.4391>. [PubMed]